Original Research *Highlight article*

Synergetic enrichment of aggrecan in nucleus pulposus cells by scAAV6-shRNA-mediated knockdown of aggrecanase-1 and aggrecanase-2

Demissew Shenegelegn Mern and Claudius Thomé

Department of Neurosurgery, Medical University of Innsbruck, Innsbruck 6020, Austria
Corresponding author: Demissew Shenegelegn Mern. Email: demissew.shenegelegn@i-med.ac.at

Impact Statement

Degenerative disk disease (DDD) causes structural damage on intervertebral disks (IVDs). DDD plays critical roles in maintenance of spinal function and health. It decreases the level of health status and raises costs for health care, social and economic affairs. Current surgical or pharmacological therapies cannot repair the structure and function of IVDs. Therefore, we established new biological repair strategies of DDD by identifying the fitting serotype of adeno-associated virus (AAV6) and shRNAs that specifically target aggrecanase-1 or aggrecanase-2. Unlike lentiviral or adenoviral gene delivery systems, AAVs do not express any viral protein. Accordingly, the use of AAVs in IVDs close to complex neural organization could diminish adverse effects that could result in neurological disorders. Our result of self-complementary adeno-associated virus grade 6 small helix ribonucleic acid (scAAV6-shRNA)-mediated combined inhibition of the key aggrecanases in nucleus pulposus (NP) cells is valuable for new therapy approaches, as it exhibited additive enrichment of aggrecan more than 56 days without any impact on NP cells.

Abstract

Degenerative disk disease (DDD) that aggravates structural deterioration of intervertebral disks (IVDs) can be accompanied by painful inflammation and immunopathological progressions. Current surgical or pharmacological therapies cannot repair the structure and function of IVDs. Nucleus pulposus (NP) cells are crucial for the preservation or restoration of IVDs by balancing the anabolic and catabolic factors affecting the extracellular matrix. Imbalanced anabolic and catabolic factors cause increased degradation of aggrecan. Aggrecanases A Disintegrin And Metalloproteinase with ThromboSpondin motifs (ADAMTS)4 and ADAMTS5 are the main degrading enzymes of aggrecan. Previously, we characterized adeno-associated virus (AAV6) as the most suitable serotype with marked NP cellular tropism and demonstrated that ADAMTS4 could be silenced by self-complementary adeno-associated virus grade 6 small helix ribonucleic acid (scAAV6-shRNA) in NP cells of degeneration grade III, which resulted in enrichment of aggrecan. Nonetheless, neither scAAV6-shRNA-mediated inhibition of ADAMTS5 nor joint inhibitions of ADAMTS4 and ADAMTS5 have been investigated, although both enzymes are regulated by analogous proinflammatory cytokines and have the same cleavage sites in aggrecan. Therefore, we attempted scAAV6-shRNA-mediated inhibitions of both enzymes in NP cells of degeneration grade IV to increase efficacies in treatments of DDD. The degeneration grade of IVDs in patients was determined by magnetic resonance imaging (MRI) before surgical operations. After isolation and culturing of NP cells, cells were transduced with scAAV6-shRNAs targeting ADAMTS4 or ADAMTS5. Transduced cells were analyzed by reverse transcription quantitative polymerase chain reaction (RT-qPCR), fluorescence microscopy, flow cytometry-assisted cell sorting (FACS), MTT assay (3-(4, 5-dimethylthiazolyl-2)-2,5-diphenyltetrazolium bromide assay), immunoblotting, and enzyme-linked immunosorbent assay (ELISA). Joint transduction of NP cells exhibited high transduction efficacies (98.1%), high transduction units (TU) (1381 TU/Cell), and no effect on cell viability or proliferation. Above all joint treatments resulted in effective knockdown of ADAMTS4 (92.8%) and ADAMTS5 (93.4%) along with additive enrichment of aggrecan (113.9%). Treatment effects were significant for more than 56 days after transduction ($P < 0.001$). In conclusion, scAAV6-shRNA-mediated combined molecular therapy could be very valuable for more effective, durable, and less immunogenic treatment approaches in DDD.

Keywords: Degenerative disk disease, biological treatment approaches, cell-based gene therapy, scAAV6-mediated inhibition of aggrecanases, combined molecular therapy in DDD, biological reconstruction of degenerative disks

***Experimental Biology and Medicine* 2023; 248: 1134–1144. DOI: 10.1177/15353702231171905**

Introduction

Painful and progressive degeneration of intervertebral disk (IVD), known as degenerative disk disease (DDD), causes structural damage on IVDs as well as chronic changes on the cartilage endplate and vertebral subchondral bone. DDD plays critical roles in maintenance of spinal function and health. It decreases the state of health and raises costs for health care, social and economic affairs.[1–6] Progressive IVD degeneration characterized by wide structural tissue

damage is commonly associated with painful inflammatory and patho-immunological courses.[7–10] Although current surgical or pharmacological therapies can offer alleviation to the accompanying suffering and disability, they cannot repair the structure and function of IVDs. As a result, they cannot stop the continuous biological decomposition of structural proteins in IVD matrix (extracellular matrix [ECM]) and the advancement of the disease into chronic disability.

Painful and progressive degeneration of IVDs including spinal instability is mostly escorted by up-regulation of inflammatory and catabolic proteins, along with the growth of nerves into the interior part of the IVDs.[7–10] Therefore, inhibition of the main inflammatory and catabolic proteins, which are responsible for structural damage and deterioration of the IVD matrix, is crucial for biological restoration of degenerative IVDs. The three major components of IVDs are nucleus pulposus (NP), annulus fibrosus (AF), and endplates (CEP, cartilaginous endplates) that are embedded in ECM. They provide the capacities of load-bearing and flexibility in the spine and are responsible for the biomechanical characteristics of the spine. CEP consists of a thin layer of hyaline cartilage sandwiched between individual vertebrae and IVDs. AF that surrounds the NP is made from different collagen fibrils and glycoproteins. NP is composed mainly of glycosaminoglycans, hyaluronan, and collagen II. The main glycosaminoglycan component in NP is aggrecan that is allied to hyaluronan by a link protein.[4,11] The principal indicator of IVD degeneration is aggrecan degradation, and growing aggrecan attenuation is considered as the outcome of increased proteolytic cleavage mediated by different matrix proteinases. Aggrecanases, known as A Disintegrin And Metalloproteinase with ThromboSpondin motifs (ADAMTSs), are matrix proteinases responsible for aggrecan cleavage at multiple cleavage sites. An increased aggrecanase activity is considered as the hallmark of cartilage and IVD deterioration.[12] From 19 currently known different members of ADAMTSs in humans, only ADAMT4 (aggrecanase-1) and ADAMTS5 (aggrecanase-2) have been found as the major aggrecanases in IVD degeneration.[13–15] Both ADAMTS4 and ADAMTS5 are multidomain metalloproteases that encompass several configurations of catalytic sites, through ADAMTS4 having only one thrombospondin (TSP) motif is shorter than ADAMTS5 with two TSP.[16] While ADAMTS4 is scarcely expressed in normal IVDs and its expression immensely rises with increased grade of IVD degeneration, ADAMTS5 is constitutively and highly expressed in normal and degenerated IVDs, but its expression rises languidly with increased grade of IVD degeneration.[15–18] Characterization of NP cells *in vitro* was previously performed in our studies by isolating NP cells from 88 patients of disk degeneration grade (DDG) III, IV, and V (63 lumbar IVDs and 15 cervical IVDs). During the characterization, we examined the viability, proliferation, morphology of NP cells, and the expression patterns of 28 endogenously expressed anabolic, catabolic, inflammatory, and matrix proteins in freshly isolated and three-dimensional (3D) cultured NP cells.[17,18] In all groups, viability, proliferation, and morphology of NP cells remained similar independent from gender, age, and grade of degeneration. However, progressive grades of degeneration showed significant influences on accumulation of selective NP cellular marker such as ADAMTS-4/5, MMP-1/2/3/13, interleukin (IL)-1β, IL-1R, tumor necrosis factor-α (TNF-α), and attenuation of other markers such as BMP2/4/6/7, IGF-1, TGF-β1/β3, aggrecan, and collagen II.[17–21] As a result, gene therapeutic interventions regulating the relevant bioactive factors identified *in vitro* and *in vivo* might contribute to the development of regenerative treatment approaches in DDD.

NP cells of degenerative IVDs have been shown to express increased levels of proinflammatory proteins such as IL-1α, IL-1β, and TNF-α that prompt high expression of ADAMTS4 and ADAMTS5.[17–21]

The primarily known endogenous regulator of ADAMTS4 and ADAMTS5 as an anti-catabolic factor is the tissue inhibitor of metalloproteinases-3 (TIMP3), since it inhibits IL-1α stimulated activities of ADAMTS4 and ADAMTS5 in a dose-dependent manner. However, imbalanced very low level TIMP3 and high-level ADAMTS4 and ADAMTS5 have been confirmed in degenerative IVDs, and this specifies the inadequacy of low-level TIMP3 for durable and effective inhibition of ADAMTS4 and ADAMTS5.[17,18,22,23] Consequently, additional inhibition of ADAMTS4 and ADAMTS5 is essential to achieve a significant enrichment of aggrecan in degenerative IVDs.

Therefore, we design shRNAs as therapeutic agents that can specifically knockdown the mRNA overexpressions of ADAMTS4 or ADAMTS5, and significantly enhance the level of aggrecan in degenerative NP cells. Previously, we evaluated the different serotypes of AAVs, and AAV6 was identified as the best serotype for optimal transduction of NP cells. Recently, we presented scAAV6-shRNA-mediated single knockdown of ADAMTS4, which led to effective aggrecan enhancement in NP cells that were isolated from IVDs of degeneration grade III.[24,25] However, neither scAAV6-shRNA-mediated inhibition of ADAMTS5 nor parallel inhibitions of both ADAMTS4 and ADAMTS5 have been attempted in NP cells of degenerative IVDs, although both enzymes are regulated by analogous proinflammatory cytokines and evidently have the same cleavage sites in aggrecan. Accordingly, we attempted scAAV6-shRNA-mediated single and parallel inhibitions of ADAMTS4 and ADAMTS5 in NP cells of degeneration grade IV to increase the effectiveness and durability of therapeutic approaches in DDD.

Materials and methods

Research ethics and tissue recruitment

The ethics committee of our university authorized this experimental study with human IVD tissues (Innsbruck Medical University: project AN2014-0027 333/4.24). NP tissue was acquired from lumbar IVDs of patients during surgery with informed consent. For participation in the study, patients provided a written informed consent. The selection criteria for surgical interventions involve preoperative magnetic resonance imaging (MRI) that showed lumbar disk herniation and nerve root pressing with related primary symptoms, in addition to six weeks unresponsiveness to nonoperative and conservative treatments. This study included 16 lumbar IVDs that showed Pfirman DDG IV on MRI.[26,27] The IVD samples recruited from 16 patients are presented in Table 1

(mean age of patients: 56 years, range: 41–68 years). NP cells were separately isolated from 16 patients, and 16 independent cellular samples were used for each experiment. Preoperative T2-weighted MRI of patients was used to determine the DDG. Figure 1 exemplifies a representative T2-weighted image of the samples showing a herniated IVD of DDG IV that presses on a nerve root. Nucleotomy was performed to acquire NP tissue from IVDs, and the acquired tissues were promptly brought to laboratory.

NP cell isolation and monolayer culture

Recruited NP was immediately washed in sterile phosphate-buffered saline solution (PBS) at 1000 × g (2 min). NP was separated from AF-residual based on their macroscopic morphology. Separated NP was finely minced into 2 mm^3 fragments and subsequently digested in 20 mL Dulbecco's Modified Eagle's Medium (DMEM) that contained pronase (0.02% w/v), glucose (1%), streptomycin/penicillin (1%), and fetal bovine serum (FBS, 10%) (37°C, 5% CO_2, 1 h) (Sigma-Aldrich). Digested sample was strained using aseptic 75 g nylon mesh filters and centrifuged at 1000 × g (2 min). Pellet was suspended in DMEM (20 mL) and digested with collagenase II (0.02% w/v) and hyaluronidase (100U, Sigma-Aldrich) for 180 min (37°C, 5% CO_2). The digested samples of NP tissue were again strained using the 75 g nylon mesh filters and centrifuged at 1000 × g (2 min). The pellet was again suspended in DMEM (10 mL) for culturing (37°C, 5% CO_2, 14 days) in 25 cm^2 flask (Sigma-Aldrich) by changing the DMEM every second day. Splitting of NP cells was done at 1:2 at 100% confluence using trypsin-EDTA (Sigma-Aldrich). After monolayer expansion, cryoconservation of NP cells was performed at −196°C in DMEM containing FBS (30%) and dimethyl sulfoxide (15%) (Sigma-Aldrich) for 3D culture and succeeding experimental steps.

3D NP cell culture

Alginate-3D-Cell-Culture Kit (AMSBIO) was applied based on the guideline of the producer. Shortly, calcium chloride liquid solution (5 mL) was dispensed in an aseptic glass cup (10 mL) having an aseptic stir bar. Pellet of the 1×10^5 transduced or untreated NP cells was made ready in Eppendorf-tube (1.5 mL) after three days of transduction. Then, 0.5 mL sodium alginate solution (0.5 mL) was dispensed into the tube containing the pellet, and a uniform cell suspension was created by mixing with the pipette. After aspiration of the cell suspension into a syringe (1 mL) fixated on a plastic flexible needle, the needle was replaced by a 22G hypodermic needle to drop the cell suspension into the glass cup having the calcium chloride solution. The suspension was dropped at two drops/s into stirring calcium chloride solution in an upright position by locating the tip of the needle about 5 cm above the surface of the liquid. The stirring of the alginate beads (circa 10 min) was completed, when the coagulated beads appeared fully white. Then, a saline solution (10 mL) was added to the beads after removal of the calcium chloride solution. After incubation at reverse transcription (RT) (15 min) and removal of the saline, the alginate beads were mixed with DMEM (10 mL) and incubated at RT (10 min). After removal of DMEM, an aseptic spatula was used to scoop 10 beads and

Table 1. Lumbar intervertebral disk samples recruited from 16 patients showing disk levels, disk degeneration grade (DDG), and age/sex.

Sample	Disk level	DDG	Age/sex
1	L5/S1	IV	41/M
2	L4/L5	IV	44/F
3	L5/S1	IV	46/F
4	L4/L5	IV	49/M
5	L5/S1	IV	50/F
6	L5/S1	IV	52/M
7	L4/L5	IV	55/F
8	L4/L5	IV	56/M
9	L5/S1	IV	59/M
10	L4/L5	IV	59/F
11	L4/L5	IV	60/F
12	L4/L5	IV	62/M
13	L5/S1	IV	63/F
14	L5/S1	IV	65/M
15	L4/L5	IV	67/F
16	L4/L5	IV	68/M

DDG: disk degeneration grade.

Figure 1. A representative T2-weighted MRI image of the herniated IVD samples with DDG IV. A representative T2-weighted MRI picture presenting a herniated lumbar IVD (L4/L5) of disk degeneration grade IV (DDG IV) with nerve root compression and six weeks unresponsiveness to nonoperative and conservative treatments. Sixteen patients having a herniated lumbar IVD of DDG IV were involved in this study (mean age of patients: 56 years, range: 41–68 years).

put them into an individual 24-well plate containing fresh DMEM (2 mL); and cells in beads were cultured up to 56 days (37°C, 5% CO_2) by changing the DMEM every second day. For every sample, three independent 3D cultures were done.

NP cell decapsulation from alginate beads

To recover NP cells from alginate beads, DMEM was removed from the 24-well plate, and the beads in each well were dissolved with sodium citrate solution (1 mL) by mixing them at RT (10 min). The mixtures in the well plates were relocated to a tube (50 mL) and centrifuged at 1000 × g (2 min). The pellet was harvested and made ready for succeeding experimental steps.

Construction of recombinant scAAV6 vectors

A shuttle plasmid based on the scAAV described before (PMID (PubMed reference number): 23987130, PMID: 20649454)[28,29] was assembled with cytomegalovirus and U6 promoters to express GFP (green fluorescent protein) and shRNA, respectively. The recombinant plasmids encoding the shRNAs targeting the mRNAs of ADAMTS4 or ADAMTS5 were designed using BLOCK-iT™ RNAi Designer (ThermoFisher), and they are termed as pAAV-ADAMTS4 and pAAV-ADAMTS5, respectively. The shRNA without any target is named pAAV-Ctrl. To avoid unspecific and unintended effects at possible off-target sites of the shRNAs, we compared the target sites of the designed shRNAs to the genome database (National center for biotechnology information/basic local alignment search tool for nucleotide). During the comparing process, we avoided any off-target sequences with more than 16 consecutive base pairs of homology. The designed shRNAs were cloned in the shuttle plasmid using *BamHI* and *HindIII*. The helper plasmid pDP6rs of AAV6 was acquired from PlasmidFactory (Bielefeld, Germany). The sense sequences of the shRNAs targeting ADAMTS4 or targeting ADAMTS5 as well as the non-target shRNA are presented correspondingly:

5′-GCTCCAGGACTTCAATATTCCTTCAAGAGAGGA ATATTGAAGTCCTGGAGCTTTTT-3′
5′-GCTCACGAAATCGGACATTTATTCAAGAGATAAA TGTCCGATTTCGTGAGCTTTTT-3′
5′-CATCTTACCGAGCATGACGTTCAAGAGACGTCAT GCTCGGTAAGATGTTTTT-3′

Recombinant scAAV6 vector production and purification

To generate recombinant scAAV6 vectors, human embryonic kidney 293 (HEK293) cells were cultured using DMEM having FCS (fetal calf serum) (10%), glucose (4.5%), and penicillin/streptomycin (1%). Before transfection, the cells were passaged twice, and 5×10^6 cells were grown in culture dish (15 cm) with DMEM (20 mL) until confluence of about 80%. First, a 30 µg of pAAV-ADAMTS4 or pAAV-ADAMTS5 or pAAV-Ctrl was separately mixed with a 96 µg of pDP6rs. Transfection medium was prepared by adding 300 mm calcium phosphate (2.5 mL) to individual mixture and slightly mixing with twofold concentrated hepes buffered saline (2.5 mL) (Sigma-Aldrich). The transfection medium was dropped to the dish and incubated for 6 h (37°C, 5% CO_2), and the medium was removed and replaced by DMEM having 2% FCS. The culture medium was collected after 72 h of transfection, and cells were harvested by trypsinization and centrifuged together at 2000 × g (5 min). After resuspension of the pellet in a 2.5 mL serum-free DMEM, freeze/thaw cycles (eight sequences) were performed for each sample by rotating the tube from dry ice-ethanol bath to 37°C water bath. Each sample was then centrifuged at 8000 × g (30 min), and supernatant containing AAV was stored at −80°C for succeeding purification as previously described (PMID: 23987130).[28] Shortly, iodixanol (Sigma-Aldrich) gradient centrifugation was used to purify the AAV supernatant, and iodixanol was eliminated by flowing the iodixanol portions through PD-10 gel filtration columns (GE Healthcare). Separately, 10 portions of each 1 mL eluate were gathered, and portions 4 to 6 were united for quantification. The purified AAV particles were quantified using quantitative polymerase chain reaction (qPCR).

Quantification of purified recombinant scAAV6 vector particles by qPCR

The purified recombinant scAAV6 vector particles were quantified using qPCR, TaqMan Gene Expression Master Mix (ThermoFisher), and LightCycler 480 (Roche Applied Science). A master mix (1×), in addition to sense and antisense primers of 5′-ITR (inverted terminal repeats) (each 200 nm) as well as ITR-probe (250 nm) and template DNA (2 µL), was used in a final volume (20 µL). The ITR primers and ITR-probe are presented as follows:

5′-ITR-sense: GGAACCCCTAGTGATGGAGTT
5′-ITR-antisense: CGGCCTCAGTGAGCGAG
ITR-probe: 6FAM-CACTCCCTCTCTGCGCGCTCG-BHQ1.

The shuttle plasmid DNA was used as a standard as defined before (PMID: 20649454),[29] and three replicates of standard, negative control, and samples were used in 96-well plate. The qPCR was programmed by applying an initial denaturation step at 95°C (10 min), 40 cycles of denaturation at 95°C (15 s), and an extension at 60°C (1 min) that included a melt curve stage 65 to 95°C (increment 0.5°C). Applied Biosystems StepOne software v2.1 (Life Technologies) was used for the qPCR data analysis. For every sample, three independent qPCRs were done. A schematic drawing showing the construction of the recombinant AAV6 vector, the production and purification AAV6 viral particle, and the AAV6 transduction of NP cells is illustrated in Supplementary Figure 1.

Assessing the transduction efficacies

A total of 1×10^5 NP cells in each well of a 24-well plate (circa 50% confluence) were sown and cultured in 500 µL DMEM having FBS (1%) (24 h, 37°C, 5% CO_2). Previously, the cellular tropism of different AAV serotypes (scAAV1-8, GFP packing) and their different viral doses (5 vg/c, 50 vg/c, 500 vg/c, 5000 vg/c, 10,000 vg/c) were characterized in NP cells.[24] scAAV6 with the viral dose of 5000 vg/c was identified as the most convenient vector for transduction of NP cells, as it exhibited the highest transduction efficacy, without any impact on cell proliferation and the expression of matrix relevant

proteins.[24,25] Therefore, NP cells were transduced with AAV6-ADAMTS4 or AAV6-ADAMTS5 or AAV6-Ctrl at a dose of 5000 vg/c. Moreover, after a day of first transduction, NP cells transduced with AAV6-ADAMTS4 were additionally transduced with AAV6-ADAMTS5 at a dose of 5000 vg/c as combined transduction (AAV6-ADAMTS4/AAV6-ADAMTS5). The efficacies of transduction were assessed every second day for the first two weeks and every week until day 56 after transduction by fluorescence microscopy (AxioVert.A, Carl Zeiss). Moreover, FACS was used to evaluate transduction efficacies in 3D cultured cells on days 8, 16, 24, 32, 48, and 56 after transduction. As described by the producer, MoFlo cell sorter (FACS, Beckman Coulter) was used to analyze 1×10^5 NP cells after transduction and determine the quantity of GFP-positive cells. Shortly, a MoFlo cell sorter was applied with a 100 mm flow cell tip and a flow rate of 12,000 events per second, along with an extension wavelength of 488 nm and a laser power of 110 W. For every sample, three independent FACS quantifications with duplicate were done.

Quantification of the TU of the recombinant scAAV6 vectors

The TU (the number of recombinant scAAV6 vectors internalized into NP cells) was determined after seeding, transducing, 3D culturing, and harvesting of NP cells on days 2, 4, 8, 16, 24, 32, 48, and 56 as described above. Cell pellets were washed three times with PBS, and AAV vectors remaining on the surface of the cells were removed. Then, pellets were suspended in a final volume (100 µL) and exposed to freeze/thaw cycles (8 sequences) by rotating the tube from the dry ice-ethanol bath to 37°C water bath. Each sample was then centrifuged at 17,000 × g (5 min), and supernatants containing AAV particles were used for titration of the TU using qPCR as described above. The shuttle plasmid was used as standard in 10-fold dilutions from 10^6 to 10^3 copies/µL along with untreated cells as a background controls. For every sample, three independent qPCRs with triplicate were done.

Viability and growth rate analyses of transduced NP cells

The viability and growth rate of NP cells were determined by MTT Assay Kit (3-(4, 5-dimethylthiazolyl-2)-2,5-diphenyltetrazolium bromide assay, ThermoFisher). The viability and proliferation rate of transduced and 3D cultured NP cells were quantified before transduction and on days 2, 4, 8, 16, 24, 32, 48, and 56 after transduction. The seeding, transducing, culturing, and harvesting of the cells are described above. Untreated cells were applied as background controls. Pellets of NP cells were washed twice with PBS and suspended in DMEM (250 µL), and duplicates of 100 µL were plated into a flat-bottomed 96-well plate. Additional control wells (only with DMEM) were used to run the blanks for absorbance readings. Following recovery incubation (37°C, 5% CO_2, 24 h), MTT substance (10 µL) was dropped to every well and further incubated (3 h). After that SDS-HCl (100 µL) was dropped to every well for extended incubation (4 h). A microtiter plate reader Infinite 200 (TECAN) was applied to determine the absorbance at 570 nm. The mean value of the blank duplicate readings was subtracted from the mean values of the sample duplicate readings. A standard curve was used to calculate the number of viable cells. For every sample, three independent MTT assays with duplicate were done.

Real-time reverse transcription quantitative PCR analysis

Real-time reverse transcription quantitative polymerase chain reaction (RT-qPCR) was applied to analyze the impact of the recombinant vectors AAV6-ADAMTS4 or AAV6-ADAMTS5 or a combination thereof (AAV6-ADAMTS4/AAV6-ADAMTS5) on the mRNA levels of ADAMTS4, ADAMTS5, and aggrecan. The seeding, transducing, culturing, and harvesting of NP cells on days 8, 16, 24, 32, 48, and 56 after transduction were described above. RNeasy Plus Mini Kit (Qiagen) was used to isolate the whole RNA, and DNase I (Sigma-Aldrich) was added to avoid DNA contamination. Biospectrometer (Eppendorf) was applied at 260 nm to quantify the isolated RNA. RT was done using equal amounts of RNA, and cDNAs were produced by the use of TaqMan Reverse Transcription Reagents (ThermoFisher). The TaqMan gene expression assays and LightCycler 480 were used to quantify mRNA levels of ADAMTS4, ADAMTS5, and aggrecan using qPCR as described above. Beta-actin was used as internal standard. Untreated NP cells were used as control. The data of relative mRNA levels were numerically presented using the comparative $2^{-\Delta\Delta CT}$ method. For every sample, three independent RT-qPCRs with triplicate were done.

The primers and probes for RT-qPCRs are presented as follows:

ADAMTS4-sense: ACATGCTGCACGACAACAGC
ADAMTS4-antisense: GTAGCCGTTGTCCAGGAAGT
ADAMTS4-probe: 6FAB-AGCACCAGCAGGCACGTGAT-BHQ1
ADAMTS5-sense: CATGAGGAGCACTACGATGC
ADAMTS5-antisense: TCAATCACAGCACAGCTGCG
ADAMTS5-probe: 6FAB-CATGTGACACCCTGGGAATG-BHQ1
Aggrecan-sense: AGGGACACCAACGAGACCTA
Aggrecan-antisense: GGAAGGTGAACTTCTCGGGG
Aggrecan-probe: 6FAB-GTACTGCTTCGCCGAGGAGA-BHQ1
Beta-actin-sense: CAGAAGGACAGCTACGTGGG
Beta-actin-antisense: CATGTCGTCCCAGTTGGTCA
Beta-actin-probe: 6FAB-GACCCTGAAGTACCCCATCG-BHQ1

Immunoblot analysis

Immunoblotting was used to investigate the impact of AAV6-ADAMTS4 or AAV6-ADAMTS5 or a combination thereof (AAV6-ADAMTS4/AAV6-ADAMTS5) on ADAMTS4, ADAMTS5, and aggrecan at protein level. The seeding, transducing, culturing, and harvesting of NP cells on days 8 and 56 after transduction were described above. Untreated NP cells were used as controls. Radio-immunoprecipitation assay (RIPA) buffer with protease and phosphatase inhibitors (Sigma-Aldrich) was used to lyze the harvested cells (4°C, 20 min). Total protein was isolated by centrifugation at 14,000 × g (4°C, 10 min), and supernatants containing protein were used for immunoblot analysis. To determine protein concentration, BCA (bicinchoninic acid) Protein Assay

Kit (ThermoFisher) was applied. Sodium dodecyl sulfate–polyacrylamide gel electrophoresis (SDS-PAGE) was used to separate proteins based on their molecular weight and transfer them to polyvinylidene fluoride (PVDF) membrane (ThermoFisher). ADAMTS4 polyclonal antibody (PA1-1749A), ADAMTS5 polyclonal antibody (PA5-27165), aggrecan polyclonal antibody (PA1-1746), and beta-actin polyclonal antibody (PA5-78715) from ThermoFisher were used as primary antibodies. Goat anti-rabbit IgG (horseradish peroxidase) (31466) and Pierce ECL Plus Western Blotting Substrate (32132X3) from ThermoFisher were used to detect the antigens on the membrane. The bands of the antigens were quantified using the software Image J. For every sample, three independent immunoblotting analyses were done.

Enzyme-linked immunosorbent assays

ELISA was used to examine the specificity of the ADAMTS4 and ADAMTS5 knockdowns as well as the enrichment of aggrecan mediated by the recombinant vectors AAV6-ADAMTS4 or AAV6-ADAMTS5 or a combination thereof AAV6-ADAMTS4/AAV6-ADAMTS5. The seeding, transducing, culturing, and harvesting of NP cells as well as isolation and quantification of total protein on days 8 and 56 after transduction were described above. Untreated NP cells were used as controls. ELISA was made for each sample with 100 µg of total protein by applying ELISA kits (Uscn Life Science Inc). Beyond the protein levels of ADAMTS4, ADAMTS5, and aggrecan, the levels of key catabolic cytokines in NP cells, such as IL-1β and TNF-α, as well as the vital tissue protein in NP, collagen type II, were quantified. To determine the absorbance of the samples at 450 nm with wavelength correction set to 540 nm, a microplate reader Infinite 200 (TECAN) was applied. The mean values of the blank duplicate readings were subtracted from the mean values of the sample duplicate readings. A standard curve was used to calculate the concentration of proteins. For every sample, three independent ELISAs with duplicate were done.

Statistical data analysis

The inter-rater reliability on MRI evaluations of DDG was determined by interpretation of kappa (κ) statistic and agreement percentage between two raters.[26,27] IBM SPSS Statistics 22 (Armonk New York USA) was applied for statistical data analyses. One-way ANOVA and pairwise comparison were applied to compare the data of transduced and untreated samples. Significance was set at $P < 0.01$.

Results

MRI grading reliability of DDG

The T2-weighted MRI-based rating of DDG was carried out by the inter-rater reliability agreement between two raters. The agreement percentage between the raters was 100% ($\kappa = 1.00$).

Recombinant scAAV6 particles quantified by qPCR

The recombinant scAAV6 genome copies were quantified by qPCR as described in "Materials and Method" section, and high final titers between 6.6×10^{11} and 2.8×10^{12} copies were quantified for all recombinant scAAV6 vectors.

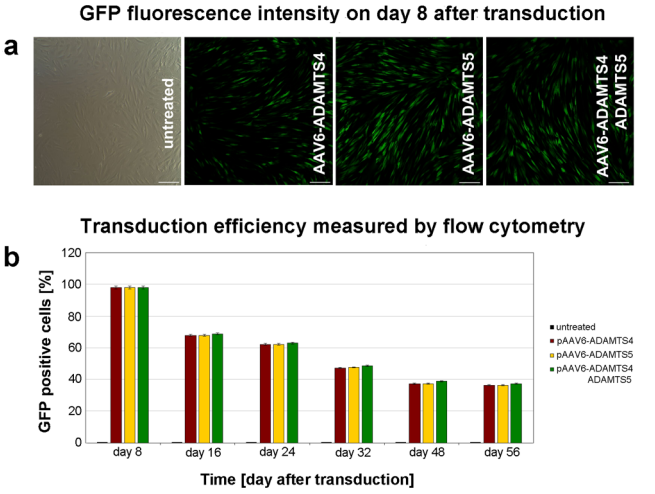

Figure 2. Transduction efficacies of recombinant scAAV6. A total of 1×10^5 NP cells were sowed in 24-well plate and cultured for 24 h in 500 µL DMEM having 1% FBS. Cells were transduced with 5000 vg/c GFP packing recombinant vector: 5000 vg/c AAV6-ADAMTS4 (encoding the shRNA targeting ADAMTS4) or 5000 vg/c AAV6-ADAMTS5 (encoding the shRNA targeting ADAMTS5) or 5000 vg/c AAV6-ADAMTS4 plus 5000 vg/c AAV6-ADAMTS5 as described in the "Method" section. Comparable transduction efficiencies were determined for all recombinant scAAV6 vectors using fluorescence microscopy and FACS. Fluorescence micrographs were obtained every second day for the first two weeks and every week until 56 days, and the maximum transduction efficacies were verified on day 8 after transduction (a), scale bars: 200 µm. For accurate quantification and presentation of the transduction efficacies by FACS, the number of GFP-positive cells was determined on days 8, 16, 24, 32, 48, and 56 after transduction (b). The amount of 1×10^5 NP cells per sample was applied to FACS analysis. Data signify mean with SD of three independent experiments.

Transduction efficiencies of recombinant scAAV6 determined by microscopy and FACS

In fluorescence microscopy, the recombinant scAAV6 vectors steadily displayed comparable transduction efficacies and their peak transduction efficacies were verified on day 8 after transduction (Figure 2(a)). Furthermore, equivalent numbers of GFP-positive cells were detected by FACS analyses. Similarly, FACS analyses showed peak transduction efficacies on day 8 with mean values of 98 (98,000 ± 787), 97.9 (97,912 ± 965), and 98.1% (98,180 ± 961) GFP-positive cells after transduction with AAV6-ADAMTS4 or AAV6-ADAMTS5 or a combination thereof AAV6-ADAMTS4/AAV6-ADAMTS5, respectively. However, on day 8 after transduction continuously decreasing numbers of GFP-positive cells were detected in the course of 56 days (Figure 2(b)). On day 56 after transduction, FACS analyses showed mean values of 36.4 (36,413 ± 423), 36.5 (36,574 ± 541), and 37.4% (37,401 ± 644) GFP-positive cells, respectively. The amount equal to 1×10^5 NP cells per sample that was applied to FACS analysis is set as 100%. Age and gender had no any effect on transduction efficacy.

Assessing the number of internalized recombinant scAAV6 in NP cells

Since only a portion of the viral particles are able to get inside the cells, quantifying the number of internalized viral particles (TU) is critical to achieve repeatable and efficient

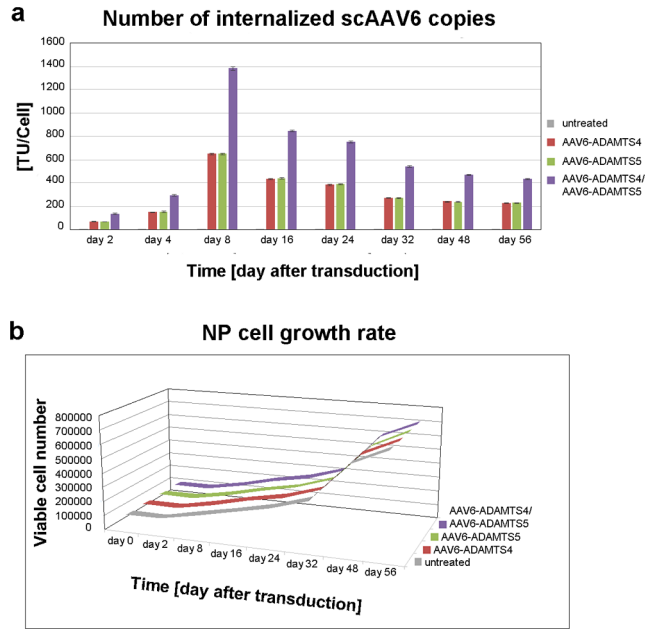

Figure 3. Internalized recombinant AAV6 copies and growth rate of NP cells. A total of 1×10^5 NP cells were transduced with recombinant vectors: 5000 vg/c AAV6-ADAMTS4 (encoding the shRNA targeting ADAMTS4) or 5000 vg/c AAV6-ADAMTS5 (encoding the shRNA targeting ADAMTS5) or a combination thereof (5000 vg/c AAV6-ADAMTS4 plus 5000 vg/c AAV6-ADAMTS5). After transduction, the number of internalized recombinant AAV6 copies (TU/Cell) and cell growth rate were determined on days 2, 8, 16, 24, 32, 48, and 56 using qPCR and MTT assay. Similar TU/Cell was confirmed for each individual transduction with augmented TU/Cell for combined transduction (a). Moreover, similar growth rates were determined for all transduced and untreated NP cells (b). Data signify mean with SD of three independent experiments.

results. TU per NP cell (TU/Cell) was evaluated for each recombinant scAAV6 vector using qPCR as described in the "Method" section, and similar TU per cell were confirmed for each individual vector. It has attained its maximum within 8 days after transduction with mean TU 646 ± 4.64 TU/Cell, 649 ± 7.11 TU/Cell, and 1381 ± 16.76 TU/Cell for AAV6-ADAMTS4 or AAV6-ADAMTS5 or combined AAV6-ADAMTS4/AAV6-ADAMTS5-transduced cells, respectively. However, in the course of the 56 days of cell culture, the TU per cell were steadily falling after day 8 of transduction. The TU on day 56 dropped to the mean values of 227.5 ± 2.88 TU/Cell, 228 ± 7.5 TU/Cell, and 434.5 ± 4.43 TU/Cell, respectively (Figure 3(a)). The combined transduction consistently showed augmented TU/Cell ($P < 0.001$). Age and gender had no any effect on TU/Cell.

Evaluating the impact of recombinant scAAV6 on cell viability and growth rate

To inspect the possible impact of recombinant scAAV6 vectors on cell viability and growth rate, 1×10^5 NP cells were seeded, cultured, and evaluated by MTT assays on days 2, 8, 16, 24, 32, 48, and 56 after transduction as described in the "Method" section. Comparable cell viabilities and growth rates were verified with all recombinant scAAV6 vectors. The results of transduced and untreated NP cells were similar. On day 56, the mean quantified number of viable cells was $712{,}007 \pm 3417$, $709{,}781 \pm 3216$, $708{,}715 \pm 2837$, and $710{,}177 \pm 2716$ for untreated cells and for AAV6-ADAMTS4 or AAV6-ADAMTS5 or AAV6-ADAMTS4/AAV6-ADAMTS5 treated cells, respectively (Figure 3(b)). Age and gender had no any effect on viability and growth rate of NP cells.

Targeted knockdown of ADAMTS4 and ADAMTS5 using scAAV6-shRNAs

The functional application of the recombinant scAAV6 vectors that encode shRNAs targeting the mRNAs of ADAMTS4 or ADAMTS5 was examined using real-time RT-qPCR. The knockdown of ADAMTS4 was achieved by AAV6-ADAMTS4 vector and knockdown of ADAMTS5 by AAV6-ADAMTS5 vector. Furthermore, parallel knockdown of ADAMTS4 and ADAMTS5 was achieved by sequential transductions of NP cells using both AAV6-ADAMTS4 and AAV6-ADAMTS5 vectors. As compared with untreated NP cells with unaffected ADAMTS4 and ADAMTS5 expression levels up to day 56, in the course of 56 days of post-transduction, maximum knockdowns of ADAMTS4 and ADAMTS5 were confirmed on post-transduction day 8. On day 8, a mean maximum ADAMTS4 reduction level of 93.0% and a mean maximum ADAMTS5 reduction level of 93.6% were determined in AAV6-ADAMTS4 transduced or AAV6-ADAMTS5-transduced NP cells, respectively. Similarly, a mean maximum ADAMTS4 reduction level of 92.8% and a mean maximum ADAMTS5 reduction level of 93.4% were determined in NP cells that were sequentially transduced with both recombinant vectors. However, the knockdown effects were continuously declining in the course of 56 days. On day 16, the mean mRNA level of ADAMTS4 was reduced to 76.4% and on day 56 to 29.2% in AAV6-ADAMTS4-transduced NP cells, and similarly, the mean mRNA level of ADAMTS5 was reduced to 74.8% on day 16 and to 32.1% on day 56 in AAV6-ADAMTS5-transduced NP. Moreover, in NP cells that were transduced with both recombinant vectors the mean mRNA levels of ADAMTS4 and ADAMTS5 were similarly reduced to 77.9 and 74.7% on day 16 and to 30.1 and 31.2% on day 56, respectively (Figure 4(a) and (c)). In addition, the maximum knockdown effects on ADAMTS4 and ADAMTS5 on day 8 of post-transduction are presented at protein level using immunoblotting (Figure 4(b) and (d)). Age and gender had no any effect.

Enrichment of aggrecan through knockdown of ADAMTS4 and ADAMTS5

Using ELISA and immunoblotting, the scAAV6-shRNA-mediated knockdown effects on aggrecan enrichment were determined at protein level. As compared with untreated NP cells with unaffected aggrecan expression levels up to day 56, the transduction of NP cells with AAV6-ADAMTS4 could increase the protein level of aggrecan at a mean maximum value of 51.6% on day 8 after transduction; the transduction with AAV6-ADAMTS5 could increase the level of aggrecan at a mean maximum value of 35.6%. Furthermore, the transduction of NP cells with both AAV6-ADAMTS4 and AAV6-ADAMTS5, which resulted in parallel knockdown of ADAMTS4 and ADAMTS5, could additively increase the level of aggrecan at a mean maximum value of 113.9% on day 8 after transduction ($P < 0.001$). However, the continuous weakening of ADAMTS4 and ADAMTS5 knockdown in the course of 56 days could also weaken the level of aggrecan

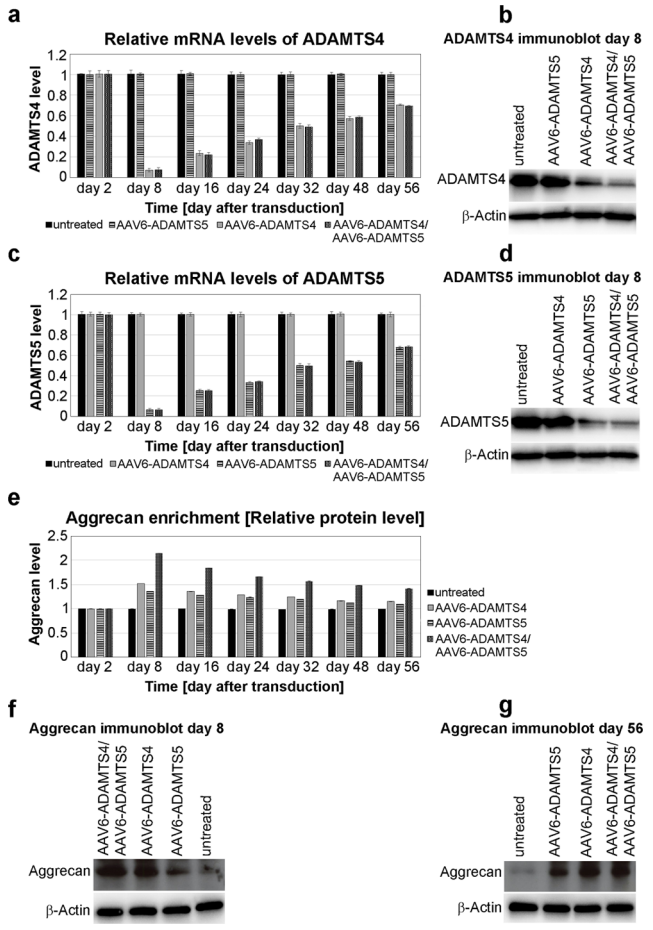

Figure 4. ADAMTS4 and ADAMTS5 knockdown using scAAV6-shRNAs and enrichment of aggrecan. A total of 5000 vg/c AAV6-ADAMTS4 (encoding the shRNA targeting ADAMTS4) or 5000 vg/c AAV6-ADAMTS5 (encoding the shRNA targeting ADAMTS5) or a combination thereof 5000 vg/c AAV6-ADAMTS4 plus 5000 vg/c AAV6-ADAMTS5 were used to transduce 1×10^5 NP cells. After harvesting of NP cells on days 2, 8, 16, 24, 32, 48, and 56, RT-qPCR and immunoblotting were completed to evaluate the knockdown effects on mRNA and protein levels of ADAMTS4 and ADAMTS5 (a and c) (b and d). The levels of ADAMTS4 and ADAMTS5 in untreated NP cells remained unaffected up to day 56 and represent the arbitrary unit 1.0, while the corresponding transductions exhibited efficient and long-dated knockdown of ADAMTS4 and ADAMTS5, respectively. Similarly, on days 2, 8, 16, 24, 32, 48, and 56 after transduction, cells were harvested to determine the protein level of aggrecan using ELISA, as presented as a ratio value (e), and immunoblotting (f and g). The levels of aggrecan in untreated cells remained unaffected up to day 56 and they represent the arbitrary unit 1.0, while the transduced NP cells showed effective and durable enrichment of aggrecan. The parallel knockdown of both ADAMTS4 and ADAMTS5 resulted in additive enrichment of aggrecan. Data signify mean with SD of three independent experiments performed in duplicate.

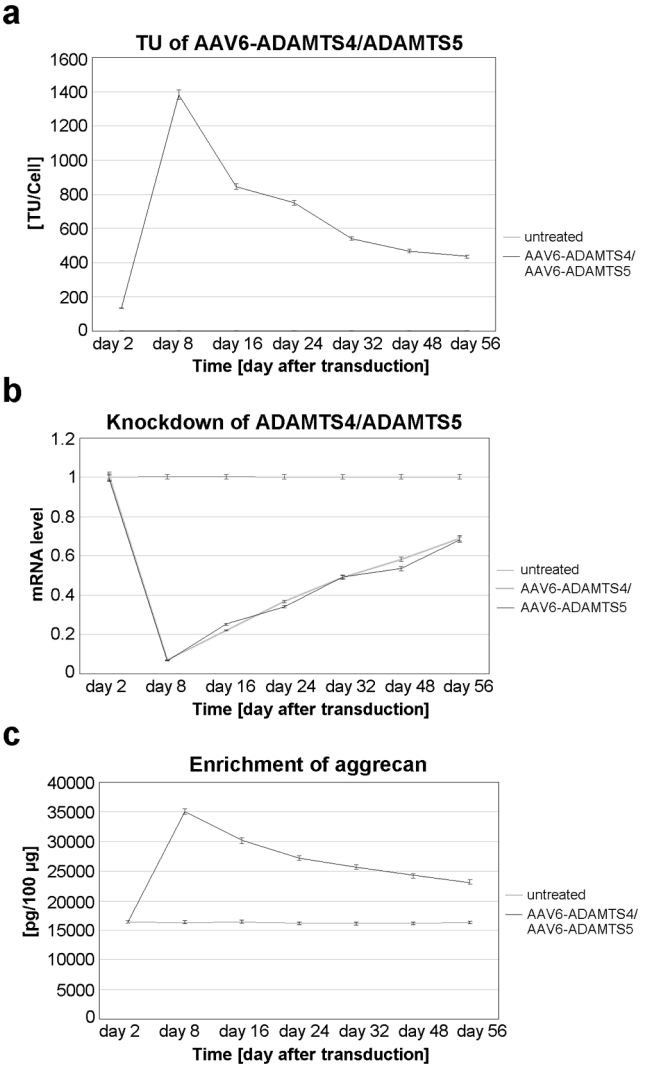

Figure 5. Correlation of TU/Cell, ADAMTS4/5-knockdown, and enrichment of aggrecan. A total of 1×10^5 NP cells that were transduced with 5000 vg/c AAV6-ADAMTS4 plus 5000 vg/c AAV6-ADAMTS5 were harvested on days 2, 8, 16, 24, 32, 48, and 56 after transduction. TU/Cell (Figure 5(a)) and mRNA levels of ADAMTS4 and ADAMTS5 (Figure 5(b)) were determined using RT-qPCR, and protein levels of aggrecan were determined using ELISA (Figure 5(c)). Transduced NP cells showed direct correlation between TU/Cell, knockdown of ADAMTS4 and ADAMTS5 along with the enrichment of aggrecan. Their levels were not affected in untreated cells. Data signify mean with SD of three independent experiments.

enrichment in similar manners. On days 16 and 56, the mean levels of aggrecan were increased only by 35.5 and 14.5% in AAV6-ADAMTS4-transduced NP cells, and by only 27.8 and 9.7% in AAV6-ADAMTS5-transduced NP cells, respectively. Nonetheless, additive enrichment of aggrecan was achieved in NP cells, which were transduced with both recombinant vectors. Their mean levels of aggrecan were increased by 83.9% on day 16 and by 41% on day 56 of post-transduction ($P < 0.001$) (Figure 4(e)). In addition, effective and durable enrichment of aggrecan is presented using immunoblotting on days 8 and 56 of post-transduction (Figure 4(f) and (g)). Age and gender had no any effect.

Knockdown specificity and its direct correlation with aggrecan enrichment

To ascertain whether the transduction of NP cells with AAV6-ADAMTS4 and AAV6-ADAMTS5 could specifically affect only ADAMTS4, ADAMTS5, and aggrecan levels, we, in addition, evaluated the levels of other key NP-related proteins, such as IL-1β, TNF-α, and collagen II using ELISA within 56 days of post-transduction. Related to the number of internalized AAV6-ADAMTS4 and AAV6-ADAMTS5 (TU/Cell), we verified proportionally reduced levels of ADAMTS4 and ADAMTS5; these levels again correlate directly with the levels of aggrecan enrichment. The proportional and direct association between TU/Cell, knockdown of ADAMTS4/ADAMTS5, and aggrecan enrichment is presented in Figure 5. In contrast, the levels of IL-1β, TNF-α,

Table 2. Knockdown specificity and enrichment of aggrecan.

Examined proteins	Untreated mean [pg/100 g]	AAV6-ADAMTS4 Mean [pg/100 µg]	AAV6-ADAMTS5 Mean [pg/100 µg]	AAV6-ADAMTS4/5 Mean [pg/100 µg]	Time
IL-1β	120.6	121.7	120.0	121.0	Day 8
	121.2	121.3	120.9	121.5	Day 56
TNF-α	108.6	107.9	109.8	107.8	Day 8
	108.5	108.3	108.9	108.8	Day 56
Collagen II	6293	6242	6209	6174	Day 8
	6189	6159	6201	6139	Day 56
ADAMTS4	2965	215.8	2958	213.3	Day 8
	2892	2077	2917	2061	Day 56
ADAMTS5	3821	3811	367.7	335.2	Day 8
	3789	3773	2647	2662	Day 56
Aggrecan	16,320	24,867	22,238	35,083	Day 8
	16,266	18,774	17,988	23,117	Day 56

AAV: adeno-associated virus; ADAMTS: A Disintegrin And Metalloproteinase with ThromboSpondin motifs; IL: interleukin; TNF-α: tumor necrosis factor-α; IL-1β: interleukin-1β; TNF-α: tumor necrosis factor-α; NP: nucleus pulposus; ELISA: enzyme-linked immunosorbent assay; SD: standard deviation.
To prove whether AAV6-ADAMTS4 and AAV6-ADAMTS5 unspecifically affect the levels of other vital NP-related proteins, the levels of IL-1β, TNF-α, and collagen II were additionally examined using ELISA. A total of 1×10^5 NP cells that were transduced with 5000 vg/c AAV6-ADAMTS4 plus 5000 vg/c AAV6-ADAMTS5 were harvested within 56 days after transduction, and 100 µg of total protein extracts was used for ELISA. In NP cells that were transduced with AAV6-ADAMTS4 or AAV6-ADAMTS5 or a combination thereof the levels of ADAMTS4, ADAMTS5 and aggrecan were specifically affected, where the combined transduction showed additive enrichment of aggrecan. The levels IL-1β, TNF-α, and collagen II were not affected in any of the transduced NP cells. The levels of all tested proteins remained unaffected in untreated cells. Data represent mean values with SD of three independent experiments on days 8 and 56 of post-transduction.

and collagen II were not affected in any of the transduced NP cells, which remained similar to the levels in untreated NP cells ($P \geqslant 0.658$) (Table 2). Age and gender had no any effect.

Discussion

Aggrecan is the key proteoglycan in NP of IVDs, and its degradation, primarily caused by the proteolytic activities of ADAMTS4 and ADAMTS5, is one of the core indicators of DDD. The cleavage of aggrecan at multiple sites by ADAMTS4 and ADAMTS5 is considered as the hallmark of IVD degradation during DDD.[17,18,30–32] Therefore, inhibition of ADAMTS4 and ADAMTS5 can be an important scheme for aggrecan enrichment in degenerative IVDs and alleviation of DDD. Although TIMPs are known as the endogenous inhibitors of ADAMTSs and MMPs, their low expression levels in degenerative IVDs are not sufficient to effectively inhibit ADAMTSs and decelerate the progression of DDD.[17,18,22,30,33,34] Therefore, small exogenous biomolecules that are well able to inhibit ADAMTSs are essential to achieve high efficiency in treatments DDD.[16–18,24,25,32] Thus, we designed shRNAs that specifically target the mRNAs of ADAMTS4 or ADAMTS5. The shRNAs were cloned in the scAAV6 vector system because it was previously established as the most suitable vector system for effective and durable transduction of human NP cells.[24,25,35–38] The main advantage of this system regarding DDD is based on the facts that AAVs are neither related to known human diseases nor express viral proteins. Consequently, toxicity and immunological side effects in an IVD region very close to sensitive neural structure could be diminished. As compared with the AAV system, the clinical applications of adenoviral and lentiviral systems in degenerative IVDs are critical due to the high risk of adverse side effects that may lead to acute neurological deficits.

The findings of this study showed comparable transduction efficiencies of single transduction (either AAV6-ADAMTS4 or AAV6-ADAMTS5) and sequential transductions (both AAV6-ADAMTS4 and AAV6-ADAMTS5 vectors) more than 56 days (Figure 2), which did not affect the viability and growth rate of NP cells (Figure 3(b)). Furthermore, the transductions specifically affected only the levels of ADAMTS4, ADAMTS5, and aggrecan, without any inflammatory and catabolic responses in NP cells (Table 2, Figure 5). Nevertheless, during the course of 56 days, the highest number of internalized vectors (TU/Cell) could be detected in sequentially transduced NP cells (Figure 3(a)). In line with this, the double knockdown could additively enhance the level of aggrecan, although the single knockdown of ADAMTS4 or ADAMTS5 could also significantly enhance the level of aggrecan (Figure 4). In all transduction conditions, the transduction efficacy, the TU/Cell, the knockdown effect, and the aggrecan enrichment were continuously weakened during the course of 56 days. This was in agreement with our anticipation, because recombinant scAAV6-shRNA vectors could persist episomal without integration into chromosome 19, and so they could get lost during cell division.[36,37] Nevertheless, the double knockdown was still capable to enhance the level of aggrecan by 41% on day 56 of post-transduction. Accordingly, our findings indicate that inhibition of both ADAMTS4 and ADAMTS5 is essential for effective enrichment of aggrecan and sustained biological treatment of DDD. These findings are in agreement with other studies, which showed analogous cleavage sites in aggrecan for both ADAMTS4 and ADAMTS5, along with parallel regulatory mechanisms by inflammatory cytokines, such as IL-1β and TNF-α through MAPK and NF-κB signaling.[30,31,39–52]

In conclusion, the parallel overexpression of ADAMTS4 and ADAMTS5 that aggravates the degradation of aggrecan in degenerative IVDs could be markedly diminished by scAAV6-shRNA-mediated double knockdown. The recombinant scAAV6-shRNA vectors targeting ADAMTS4 and ADAMTS5 have the potential to be used as safe and effective

gene delivery system for long-term therapeutic applications in DDD. Moreover, such modified NP cells could be beneficial for clinical application concerning cell-based regenerative therapy in DDD. In view of clinical application, a detailed investigation of possible off-target effects is very important. The application of whole genome sequencing along with deep sequencing is a convincing approach for effective identification of possible off-target effects. It could allow a clear look at the entire sites across the genome of NP cells and minimize unexpected side effects, which could be dangerous for clinical application.

AUTHORS' CONTRIBUTIONS

All authors participated in the design and interpretation of the study as well as in analysis of the data, review, and approval of the manuscript; DSM and CT conceived and designed the manuscript; DSM performed the acquisition of data; DSM and CT completed the analysis and interpretation of data; DSM wrote the manuscript; DSM and CT revised and final approved of the manuscript.

DECLARATION OF CONFLICTING INTERESTS

The author(s) declared no potential conflicts of interest with respect to the research, authorship, and/or publication of this article.

ETHICAL APPROVAL

The ethics committee of our university authorized this experimental study with human IVD tissues (Innsbruck Medical University: project AN2014-0027 333/4.24). Nucleus NP tissue was acquired from lumbar IVDs of patients during surgery with informed consent. The selection criteria for surgical interventions involve preoperative MRI that showed lumbar disk herniation and nerve root pressing with related primary symptoms, in addition to six weeks unresponsiveness to nonoperative and conservative treatments.

FUNDING

The author(s) received no financial support for the research, authorship, and/or publication of this article.

ORCID ID

Demissew Shenegelegn Mern https://orcid.org/0000-0001-5893-981X

SUPPLEMENTAL MATERIAL

Supplemental material for this article is available online.

REFERENCES

1. Peng B, Wu W, Hou S, Li P, Zhang C, Yang Y. The pathogenesis of discogenic low back pain. *J Bone Joint Surg Br* 2005;**87**:62–7
2. Kandel R, Roberts S, Urban JP. Tissue engineering and the intervertebral disc: the challenges. *Eur Spine J* 2008;**4**:480–91
3. Funabashi M, Kawchuk GN, Vette AH, Goldsmith P, Prasad N. Tissue loading created during spinal manipulation in comparison to loading created by passive spinal movements. *Sci Rep* 2016;**6**:38107
4. Adams MA, Dolan P. Spine biomechanics. *J Biomech* 2005;**38**:1972–83
5. Enthoven P, Skargren E, Oberg B. Clinical course in patients seeking primary care for back or neck pain: a prospective 5-year follow-up of outcome and health care consumption with subgroup analysis. *Spine* 2004;**29**:2458–65
6. Wenig CM, Schmidt CO, Kohlmann T, Schweikert B. Costs of back pain in Germany. *Eur J Pain* 2009;**13**:280–6
7. Burke JG, Watson RW, McCormack D, Dowling FE, Walsh MG, Fitzpatrick JM. Intervertebral discs which cause low back pain secrete high levels of proinflammatory mediators. *J Bone Joint Surg Br* 2002;**84**:196–201
8. Mulleman D, Mammou S, Griffoul I, Watier H, Goupille P. Pathophysiology of disk-related sciatica. I. Evidence supporting a chemical component. *Joint Bone Spine* 2006;**73**:151–8
9. Hoyland JA, Le Maitre C, Freemont AJ. Investigation of the role of IL-1 and TNF in matrix degradation in the intervertebral disc. *Rheumatology* 2008;**47**:809–14
10. Freemont AJ, Peacock TE, Goupille P, Hoyland JA, O'Brien J, Jayson MI. Nerve ingrowth into diseased intervertebral disc in chronic back pain. *Lancet* 1997;**350**:178–81
11. Roughley PJ. Biology of intervertebral disc aging and degeneration: involvement of the extracellular matrix. *Spine* 2004;**29**:2691–9
12. Sandy JD, Verscharen C. Analysis of aggrecan in human knee cartilage and synovial fluid indicates that aggrecanase (ADAMTS) activity is responsible for the catabolic turnover and loss of whole aggrecan whereas other protease activity is required for C-terminal processing in vivo. *Biochem J* 2001;**358**:615–26
13. Tang BL. ADAMTS: a novel family of extracellular matrix proteases. *Int J Biochem Cell Biol* 2001;**33**:33–44
14. Cal S, Obaya AJ, Llamazares M, Garabaya C, Quesada V, López-Otín C. Cloning, expression analysis, and structural characterization of seven novel human ADAMTSs, a family of metalloproteinases with disintegrin and thrombospondin-1 domains. *Gene* 2002;**283**:49–62
15. Tortorella MD, Malfait AM, Deccico C, Arner E. The role of ADAM-TS4 (aggrecanase-1) and ADAM-TS5 (aggrecanase-2) in a model of cartilage degradation. *Osteoarthritis Cartilage* 2001;**9**:539–52
16. Bondeson J, Wainwright S, Hughes C, Caterson B. The regulation of the ADAMTS4 and ADAMTS5 aggrecanases in osteoarthritis: a review. *Clin Exp Rheumatol* 2008;**26**:139–45
17. Mern DS, Fontana J, Beierfuß A, Thomé C, Hegewald AA. A combinatorial relative mass value evaluation of endogenous bioactive proteins in three-dimensional cultured nucleus pulposus cells of herniated intervertebral discs: identification of potential target proteins for gene therapeutic approaches. *PLoS ONE* 2013;**8**:e81467
18. Mern DS, Beierfuß A, Fontana J, Thomé C, Hegewald AA. Imbalanced protein expression patterns of anabolic, catabolic, anti-catabolic and inflammatory cytokines in degenerative cervical disc cells: new indications for gene therapeutic treatments of cervical disc diseases. *PLoS ONE* 2014;**9**:e96870
19. Caterson B, Flannery CR, Hughes CE, Little CB. Mechanisms involved in cartilage proteoglycan catabolism. *Matrix Biol* 2000;**19**:333–44
20. Bayliss MT, Hutton S, Hayward J, Maciewicz RA. Distribution of aggrecanase (ADAMts 4/5) cleavage products in normal and osteoarthritic human articular cartilage: the influence of age, topography and zone of tissue. *Osteoarthritis Cartilage* 2001;**9**:553–60
21. Sandy JD. A contentious issue finds some clarity: on the independent and complementary roles of aggrecanase activity and MMP activity in human joint aggrecanolysis. *Osteoarthritis Cartilage* 2006;**14**:95–100
22. Kashiwagi M, Tortorella M, Nagase H, Brew K. TIMP-3 is a potent inhibitor of aggrecanase 1 (ADAM-TS4) and aggrecanase 2 (ADAM-TS5). *J Biol Chem* 2001;**276**:12501–4
23. Gendron C, Kashiwagi M, Hughes C, Caterson B, Nagase H. TIMP-3 inhibits aggrecanase-mediated glycosaminoglycan release from cartilage explants stimulated by catabolic factors. *FEBS Lett* 2003;**555**:431–6
24. Mern DS, Thomé C. Identification and characterization of human nucleus pulposus cell specific serotypes of adeno-associated virus for gene therapeutic approaches of intervertebral disc disorders. *BMC Musculoskelet Disord* 2015;**16**:341
25. Mern DS, Tschugg A, Hartmann S, Thomé C. Self-complementary adeno-associated virus serotype 6 mediated knockdown of ADAMTS4 induces long-term and effective enhancement of aggrecan in degenerative human nucleus pulposus cells: a new therapeutic approach for intervertebral disc disorders. *PLoS ONE* 2017;**12**:e0172181

26. Pfirrmann CW, Metzdorf A, Zanetti M, Hodler J, Boos N. Magnetic resonance classification of lumbar intervertebral disc degeneration. *Spine* 2001;**26**:1873–8
27. Bangdiwala SI. Graphical aids for visualizing and interpreting patterns in departures from agreement in ordinal categorical observer agreement data. *J Biopharm Stat* 2017;**27**:773–83
28. Wagner A, Röhrs V, Kedzierski R, Fechner H, Kurreck J. A novel method for the quantification of adeno-associated virus vectors for RNA interference applications using quantitative polymerase chain reaction and purified genomic adeno-associated virus DNA as a standard. *Hum Gene Ther Methods* 2013;**24**:355–63
29. Rothe D, Wajant G, Grunert HP, Zeichhardt H, Fechner H, Kurreck J. Rapid construction of adeno-associated virus vectors expressing multiple short hairpin RNAs with high antiviral activity against echovirus 30. *Oligonucleotides* 2010;**20**:191–8
30. Tortorella MD, Pratta M, Liu RQ, Austin J, Ross OH, Abbaszade I, Burn T, Arner E. Sites of aggrecan cleavage by recombinant human aggrecanase-1 (ADAMTS-4). *J Biol Chem* 2000;**275**:18566–73
31. Tortorella MD, Liu RQ, Burn T, Newton RC, Arner E. Characterization of human aggrecanase 2 (ADAM-TS5): substrate specificity studies and comparison with aggrecanase 1 (ADAM-TS4). *Matrix Biol* 2002;**21**: 499–511
32. Mern DS, Beierfuß A, Thomé C, Hegewald AA. Enhancing human nucleus pulposus cells for biological treatment approaches of degenerative intervertebral disc diseases: a systematic review. *J Tissue Eng Regen Med* 2014;**8**:925–36
33. Wayne GJ, Deng S, Amour A, Borman S, Matico R, Carter HL, Murphy G. TIMP-3 inhibition of ADAMTS-4 (Aggrecanase-1) is modulated by interactions between aggrecan and the C-terminal domain of ADAMTS-4. *J Biol Chem* 2007;**282**:20991–8
34. Nagase H, Brew K. Designing TIMP (tissue inhibitor of metalloproteinases) variants that are selective metalloproteinase inhibitors. *Biochem Soc Symp* 2003;**70**:201–12
35. McCarty DM. Self-complementary AAV vectors; advances and applications. *Mol Ther* 2008;**16**:1648–56
36. Heister T, Heid I, Ackermann M, Fraefel C. Herpes simplex virus type 1/adeno-associated virus hybrid vectors mediate site-specific integration at the adeno-associated virus preintegration site, AAVS1, on human chromosome 19. *J Virol* 2002;**76**:7163–73
37. Grieger JC, Samulski RJ. Adeno-associated virus as a gene therapy vector: vector development, production and clinical applications. *Adv Biochem Eng Biotechnol* 2005;**99**:119–45
38. Bartlett JS, Wilcher R, Samulski RJ. Infectious entry pathway of adeno-associated virus and adenoassociated virus vectors. *J Virol* 2000;**74**: 2777–85
39. Mancheño-Corvo P, Martín-Duque P. Viral gene therapy. *Clin Transl Oncol* 2006;**8**:858–67
40. Moon SH, Nishida K, Gilbertson LG, Lee HM, Kim H, Hall RA, Robbins PD, Kang JD. Biologic response of human intervertebral disc cells to gene therapy cocktail. *Spine* 2008;**33**:1850–5
41. Lee JY, Hall R, Pelinkovic D, Cassinelli E, Usas A, Gilbertson L, Huad J, Kang J. New use of a three-dimensional pellet culture system for human intervertebral disc cells: initial characterization and potential use for tissue engineering. *Spine* 2001;**26**:2316–22
42. Hacein-Bey-Abina S, Von Kalle C, Schmidt M, McCormack MP, Wulffraat N, Leboulch P, Lim A, Osborne CS, Pawliuk R, Morillon E, Sorensen R, Forster A, Fraser P, Cohen JI, de Saint Basile G, Alexander I, Wintergerst U, Frebourg T, Aurias A, Stoppa-Lyonnet D, Romana S, Radford-Weiss I, Gross F, Valensi F, Delabesse E, Macintyre E, Sigaux F, Soulier J, Leiva LE, Wissler M, Prinz C, Rabbitts TH, Le Deist F, Fischer A, Cavazzana-Calvo M. LMO2-associated clonal T cell proliferation in two patients after gene therapy for SCID-X1. *Science* 2003;**302**:415–9
43. Wold WS, Doronin K, Toth K, Kuppuswamy M, Lichtenstein DL, Tollefson AE. Immune responses to adenoviruses: viral evasion mechanisms and their implications for the clinic. *Curr Opin Immunol* 1999;**11**:380–6
44. Wallach CJ, Sobajima S, Watanabe Y, Kim JS, Georgescu HI, Robbins P, Gilbertson LG, Kang JD. Gene transfer of the catabolic inhibitor TIMP-1 increases measured proteoglycans in cells from degenerated human intervertebral discs. *Spine* 2003;**28**:2331–7
45. Gilbertson L, Ahn SH, Teng PN, Studer RK, Niyibizi C, Kang JD. The effects of recombinant human bone morphogenetic protein-2, recombinant human bone morphogenetic protein-12, and adenoviral bone morphogenetic protein-12 on matrix synthesis in human annulus fibrosis and nucleus pulposus cells. *Spine J* 2008;**8**:449–56
46. Ilic MZ, Robinson HC, Handley CJ. Characterization of aggrecan retained and lost from the extracellular matrix of articular cartilage. Involvement of carboxyl-terminal processing in the catabolism of aggrecan. *J Biol Chem* 1998;**273**:17451–8
47. Wang M, Shen J, Jin H, Im HJ, Sandy J, Chen D. Recent progress in understanding molecular mechanisms of cartilage degeneration during osteoarthritis. *Ann N Y Acad Sci* 2011;**1240**:61–9
48. Lark MW, Gordy JT, Weidner JR, Ayala J, Kimura JH, Williams HR, Mumford RA, Flannery CR, Carlson SS, Iwata M, Sandy JD. Cell-mediated catabolism of aggrecan. Evidence that cleavage at the "aggrecanase" site (Glu373–Ala374) is a primary event in proteolysis of the interglobular domain. *J Biol Chem* 1995;**270**:2550–6
49. Tortorella MD, Pratta MA, Fox JW, Arner EC. The interglobular domain of cartilage aggrecan is cleaved by hemorrhagic metalloproteinase HT-d (atrolysin C) at the matrix metalloproteinase and aggrecanase sites. *J Biol Chem* 1998;**273**:5846–50
50. Tortorella MD, Pratta M, Liu RQ, Abbaszade I, Ross H, Burn T, Arner E. The thrombospondin motif of aggrecanase-1 (ADAMTS-4) is critical for aggrecan substrate recognition and cleavage. *J Biol Chem* 2000;**275**: 25791–7
51. Pratta MA, Tortorella MD, Arner EC. Age-related changes in aggrecan glycosylation affect cleavage by aggrecanase. *J Biol Chem* 2000;**275**: 39096–102
52. Tian Y, Yuan W, Fujita N, Wang J, Wang H, Shapiro IM, Risbud MV. Inflammatory cytokines associated with degenerative disc disease control aggrecanase-1 (ADAMTS-4) expression in nucleus pulposus cells through MAPK and NF-κB. *Am J Pathol* 2013;**182**:2310–21

(Received September 12, 2022, Accepted March 7, 2023)